Title	A comprehensive cocrystal screening study of chlorothiazide
Author(s)	Aljohani, Marwah; Pallipurath, Anuradha R.; McArdle, Patrick; Erxleben, Andrea
Publication Date	2017-09-01
Publication Information	Aljohani, Marwah, Pallipurath, Anuradha R., McArdle, Patrick, & Erxleben, Andrea. (2017). A Comprehensive Cocrystal Screening Study of Chlorothiazide. Crystal Growth & Design, 17(10), 5223-5232. doi: 10.1021/acs.cgd.7b00745
Publisher	American Chemical Society
Link to publisher's version	http://dx.doi.org/10.1021/acs.cgd.7b00745
Item record	http://hdl.handle.net/10379/7197
DOI	http://dx.doi.org/10.1021/acs.cgd.7b00745

A Comprehensive Cocrystal Screening Study of Chlorothiazide

Marwah Aljohani, Anuradha R. Pallipurath, Patrick McArdle,* and Andrea Erxleben*

School of Chemistry, National University of Ireland, Galway, Ireland

*Corresponding author email address: andrea.erxleben@nuigalway.ie (AE);

p.mcardle@nuigalway.ie (PM)

Abstract

Cocrystal formation of chlorothiazide (ctz) was screened with a variety of coformers with carboxyl, amide, hydroxyl, sulfonamide, pyridine, amidine and amine functional groups. New cocrystals with acetamide (aca), benzamide (bza), propionamide (ppa), caprolactam (cap), carbamazepine (cbz), nicotinamide (nia), isonicotinamide (ina), hexamethylenetetramine (hma), 4,4'-bipyridine (bipy), 1,2-di(4-pyridyl)ethylene (ebipy), 2-hydroxypyridine (hyp), 1,3-di(4-pyridyl)propane (pbipy) and pyrazine (pyr) as well as a benzamidinium ($bzamH^+$) salt were obtained by mechanical grinding and liquid-assisted grinding and identified by X-ray powder diffraction. The structures of ctz-bza, ctz-cbz, ctz-ina, ctz-nia, ctz-hma, ctz-bipy, ctz-ebipy, ctz-pbipy and ($bzamH^+$)(ctz^-) were determined by single-crystal X-ray diffraction. Analysis of the hydrogen bonding motifs showed that in all cocrystal structures except for ctz-bipy, the $NH_{sulfonamide}\cdots N(SO_2)=C$ catemer synthon of ctz form I is replaced by ctz-coformer heterosynthons. The dissolution behavior and relationship between dissolution rate, packing index and lattice energy of the cocrystals is described. To understand why no cocrystals with carboxylic acids formed, a motif search of the Cambridge Structural Database (CSD) was carried out.

Keywords: Chlorothiazide, cocrystal, dissolution rate, hydrogen bonding, sulfonamide

Introduction

The preparation of new multicomponent molecular crystals by cocrystallization of an active pharmaceutical ingredient (API) and a biologically safe coformer is a well-established concept for optimizing the physicochemical and mechanical properties of an API such as the dissolution rate, bioavailability, particle size, particle morphology, tabletability and compactability, without making

chemical modifications to the drug molecule.[1-4] Cocrystals as new solid-state forms also offer opportunities for patent protection and thus can be of significant commercial value.[5]

The crystal engineering approach which uses supramolecular heterosynthons between the API and the coformer is an effective strategy for the rational selection of suitable coformers and the design of new pharmaceutical cocrystals.[6,7] It is thus important to understand the hydrogen bonding interactions that lead to robust heterosynthons in the cocrystal compared to the homosynthons in the individual components. Although the sulfonamide group is the common functional group in the important class of sulfa drugs and its hydrogen bonding preferences have been investigated,[8] relatively few studies have been concerned with the propensity of sulfonamides to cocrystal formation. In fact, examples for cocrystals of sulfa drugs have been published only recently.[9-18] In several of the reported sulfa drug cocrystals the sulfa drug contains a 2-pyridyl, 2-thiazole or 2-pyrimidyl substituted sulfonamide group and the supramolecular synthons involve the heterocyclic nitrogen (*e.g.* formation of the $R_2^2(8)$ motif through pairs of $NH_{sulfonamide}\cdots O_{carboxyl}$ and $OH_{carboxyl}\cdots N_{pyridine}$ hydrogen bonds in carboxylic acid cocrystals).[10,12,13,18]

Chlorothiazide (ctz, 6-chloro-4*H*-1,2,4-benzothiadiazine-7-sulfonamide 1,1-dioxide) is a short-acting thiadiazine diuretic. It is applied in edema caused by various forms of renal dysfunction and is used to manage excess fluid linked to congestive heart failure. It also has a secondary function as an antihypertensive.[19] Ctz is a cyclic secondary sulfonamide that also contains a primary SO_2NH_2 substituent and that can exist in two tautomeric forms (Figure 1). Here we report the results of an extensive cocrystal screening study of ctz with a variety of coformers. The crystal structures of eight new cocrystals and a salt are described along with an analysis of heterosynthon formation and hydrogen bonding preferences of the sulfonamide groups in ctz.

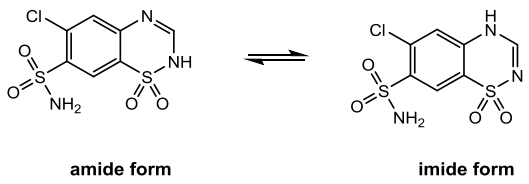

Figure 1. Tautomeric forms of chlorothiazide.

Materials and Methods

Materials. Ctz and nicotinamide (nia) were purchased from Tokyo Chemical Industry (TCI, Europe). The coformers 4,4'-bipyridine (bipy), 1,3-di(4-pyridyl)propane (pbiby), 1,2-di(4-pyridyl)ethylene

(ebipy), benzamidine (bzam), hexamethylenetetramine (hma), isonicotinamide (ina), nicotinamide (nia), propionamide (ppa), deoxycholic acid (dca**)**, and sodium deoxycholate (NaDc) were purchased from Sigma Aldrich. Carbamazepine (cbz) and benzamide (bza) were purchased from Alfa Aesar.

Ball milling. Room temperature milling experiments were performed using an oscillatory ball mill (Mixer Mill MM400, Retsch GmbH & Co., Germany) and a 25 mL stainless steel milling jar containing one 15 mm diameter stainless steel ball. The ctz : coformer molar ratio was 1 : 1 (0.5 g sample in total) except for cbz, where a 1 : 2 molar ratio was used. The samples were milled at 25 Hz for 60 min. with a cool down period of 15 min after 30 min. The milled powder samples were analyzed immediately by powder X-ray diffraction. When no cocrystal formation was observed, 100 µL of acetonitrile was added to the milling jar prior to milling. Cryo-milling of ctz/dca (1 : 1) was carried out by immersing the jars initially in liquid nitrogen for 5 min. After every 7.5 min. of milling the sample was cooled again in liquid nitrogen for 2.5 minutes. The measured external temperature of the jars did not rise above -20 °C during cryo-milling. To monitor the recrystallization of the amorphous samples, samples were stored in a desiccator (sealed using silica gel) at ambient temperature (22 ±2 ^{o}C) under 56 % relativity humidity which was achieved using a solution of $Ca(NO_3)_2$.[20] The stored samples were analyzed after 1, 3, 7, 15, 30 and 60 days by X-ray powder diffraction.

Solution crystallization. In separate vials ctz (50 mg, 0.17 mmol) and 1 or 2 equivalents of the respective coformer were dissolved in a minimum amount of solvent. Dissolution was aided by heating or sonication. Then the clear solutions were mixed and left to slowly evaporate at room temperature or 4 °C. In the case of bipy, ebipy, pbipy, hma, bza, cbz, ina, nia and bzam X-ray suitable single crystals were obtained within a week.

Ctz-bipy: 1:2 molar ratio, acetone, room temperature; ctz-ebipy: 1:2 molar ratio, acetone, room temperature; ctz-pbipy: 1:1 molar ratio, acetone, room temperature; ctz-hma: 1:2 molar ratio, acetonitrile, room temperature; ctz-bza: 1:2 molar ratio, acetone, room temperature; ctz-cbz: 1:2 molar ratio, acetone, room temperature; ctz-ina: 1:2 molar ratio, acetonitrile, room temperature; ctz-nia: 1:2 molar ratio, acetonitrile, room temperature; $(bzamH^+)(ctz^-)$: 1:1 molar ratio, acetonitrile, 4 °C.

Differential scanning calorimetry. A STA625 thermal analyser from Rheometric Scientific (Piscataway, New Jersey) was used to perform thermal analysis. The heating rate was 10 °C/min and the runs were performed between 25 °C and 400 °C. Open aluminium crucibles were used, nitrogen was purged in the ambient mode and an indium standard was used for calibration.

IR spectroscopy. FT-IR spectra were recorded on a Perkin Elmer Spectrum 400 fitted with an ATR reflectance attachment. Spectra were collected in the 650 − 3600 cm^{-1} range with a resolution of 4 cm^{-1} and four integrated scans on a diamond/ZnSe window.

Dissolution studies. The powder sample (100 mg) was placed in 250 mL 0.1 M phosphate buffer (pH 6.8, 37 °C) and stirred at 300 rpm with an 11-mm magnetic stirring bar. Aliquots of 2.5 mL were withdrawn at predetermined time points (1, 2, 5, 10, 15, 25, 30, 45, 60, 90, 120, and 180 min.) and immediately replaced with 2.5 mL of dissolution medium. The samples were each diluted by adding 4.75 mL dissolution medium and were analyzed on the same day using UV/Vis spectroscopy. All dissolution experiments were performed in triplicate. The amount of dissolved ctz was determined with a Varian Cary 50 Scan Spectrophotometer (Santa Clara, CA, USA). To exclude any interference due to absorption of the coformer, reference spectra were recorded for the buffer solution and the buffer solution containing either of the coformers. The concentrations of ctz were measured at 325 nm. Standard solutions (0.0500, 0.0375, 0.025, 0.0125, 0.005, 0.0025, 0.0005 and 0.0001 mg/mL ctz) were prepared with phosphate buffer (0.1 M, pH 6.8). In the relevant concentration range the calibration curve was linear ($R^2 = 0.9998$).

X-ray powder diffraction. X-ray powder patterns of samples obtained by mechanical grinding and crystallization from solution were recorded on an Inel Equinox 3000 powder diffractometer between 5 and 90 ° (2θ) using Cu K_α radiation (λ = 1.54178 Å, 35 kV, 25 mA). Theoretical powder patterns for the cocrystals analyzed by single crystal X-ray analysis were calculated using the OSCAIL software package.[21]

Crystal structure determination and refinement. Single crystal diffraction data were collected on an Oxford Diffraction Xcalibur CCD diffractometer at room temperature using graphite-monochromated Mo-Kα radiation (λ = 0.71073 Å). The structures were solved by direct methods and subsequent Fourier syntheses and refined by full-matrix least squares on F^2 using SHELXT,[22] embedded in the OSCAIL software.[21] Graphics were produced with ORTEX and POGL also embedded in OSCAIL. Crystallographic data and details of refinement are reported in Tables 1 and 2. CIF files can be obtained free of charge at www.ccdc.cam.ac.uk/conts/retrieving.html or from the Cambridge Crystallographic Data Centre, Cambridge, UK with the REF codes 1551836 (ctz-bipy), 1551880 (ctz·dmf), 1551879 (ctz-bza), 1551881 (ctz-pbipy), 1551885 (ctz-ebipy), 1551886 (ctz-cbz), 1551887 (ctz-hma), 1551888 (ctz-ina), 1551889 (ctz-nia), 1551899 ($(bzamH^+)(ctz^-)$).

CSD motif search. A motif search for the types of H-bonded adducts shown in Figure 2 was carried out, using the Conquest software.[23] The criteria used for the search were similar to that of our previous study,[24] where the interactions within a distance of the sum of the vdW radii and structures with an R-factor < 7.5% were considered and organometallics were excluded.

Computational studies. Density Functional Theory (DFT) calculations were made using Firefly version 8.2.0 with B3LYP functionals and 6-31G* basis sets.[25]

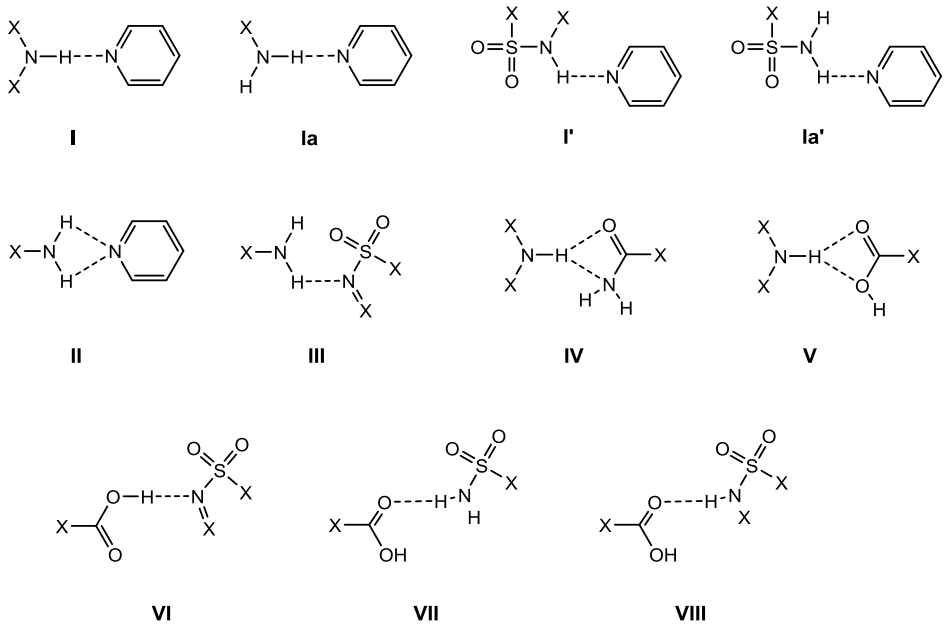

Figure 2. Motifs included in the CSD motif search.

Results and Discussion

Cocrystal formation with a range of coformers with different functional groups including carboxyl, amide, hydroxyl, amidine, sulfonamide, amine, and pyridyl groups was screened using mechanical and liquid-assisted grinding. The advantage of mechanochemical methods is that the success of cocrystal formation is unaffected by solubility differences which during solution crystallization experiments may lead to the individual crystallization of the least soluble component. With the aim of carrying out a detailed investigation of hydrogen bonding preferences, GRAS (generally regarded as safe) as well as non-GRAS model coformers were studied. All ctz-coformer mixtures (1:1 ratio unless stated otherwise) were ball-milled for 60 min. in the absence and presence of a catalytic amount of acetonitrile or acetone and analyzed by X-ray powder diffraction (XRPD). The coformers used and the results of the milling experiments are listed in Table S1 in the Supporting Information (SI). Surprisingly, none of the 15 carboxylic acids tested formed a cocrystal with ctz. Likewise, the XRPD patterns of neat- and liquid-assisted ground samples of ctz and another sulfonamide (sulfanilamide) showed a physical mixture of the two components. Milling of ctz with carbamazepine (cbz), benzamidine (bzam), cyanuric acid (cya), hexamethylenetetramine (hma) and benzene-1,3,5-tricarboxylic acid (bta) in the absence of solvent resulted in XRPD patterns that featured an amorphous halo. The ctz-cbz and ctz-bzam samples remained X-ray amorphous for at least one month when kept in a humidity chamber under 56 % relative humidity (RH) and room temperature. Ctz-bta and ctz-cya recrystallized to the respective physical mixture within 1 and 3 days under the same

conditions. The XRPD pattern of the ctz-hma sample showed the Bragg peaks of ctz after 1d. In addition, new peaks appeared that matched those of the ctz-hma cocrystal obtained by solution crystallization (see below). When X-ray amorphous ctz-cya and ctz-bta were milled for longer times (2 h), the Bragg peaks of ctz, cya and bta re-appeared. The XRPD pattern of a ball-milled sample of ctz and deoxycholic acid (dca) showed ctz peaks with an underlying amorphous halo. When the milling was performed at low temperature (cryomilling), a fully X-ray amorphous solid was obtained that did not recrystallize for at least 1 month at room temperature and 56 % RH. Likewise, milling of ctz with sodium deoxycholate at low temperature resulted in complete amorphization. However, ctz peaks were observed after storage for two weeks.

By contrast, new XRPD patterns were obtained on neat milling with the amide and pyridine coformers acetamide (aca), benzamide (bza), caprolactam (cap), isonicotinamide (ina), 4,4'-bipyridine (bipy), 2-hydroxypyridine (hyp), 1,3-di(4-pyridyl)propane (pbipy) and pyrazine (pyr), indicating the formation of cocrystals (Figures S1 – S8). In the case of propionamide (ppa), cbz, nicotinamide (nia), hma, 1,2-di(4-pyridyl)ethylene (ebipy) and bzam new XRPD patterns were observed when traces of solvent were added prior to milling (Figures S9 – S14).

In order to analyze the H bonding motifs in the ctz cocrystals, solution crystallization experiments in acetonitrile, acetone and dimethylformamide were carried out. X-ray suitable single crystals were obtained in the case of ctz-bipy, ctz-ebipy, ctz-pbipy, ctz-hma, ctz-bza, ctz-cbz, ctz-ina and ctz-nia. In addition, the X-ray structures of the salt ($bzamH^+$)(ctz^-) and of the dimethylformamide solvate, ctz·dmf, were solved. Unfortunately, the other cocrystals identified during the grinding experiments, ctz-aca, ctz-cap, ctz-ppa, ctz-hyp and ctz-pyr, did not crystallize from solution. In fact the X-ray suitable crystals of ctz·dmf whose structure had previously been determined from XRPD data[26] were obtained during cocrystallization experiments with acetamide. Attempts to obtain single crystals of ctz-aca, ctz-cap, ctz-ppa, ctz-hyp and ctz-pyr by seeding with the ground samples resulted in micrcrystalline cocrystallization products (ctz-cap, ctz-hyp) or in the individual crystallization of ctz (aca, ppa, pyr).

The cocrystals that crystallized upon mixing concentrated solutions of ctz and the respective coformer had 1:1 (ctz-ebipy, ctz-hma, ctz-bza, ctz-ina, ctz-nia), 1:2 (ctz-pbipy, ctz-cbz) and 2:1 (ctz-bipy) stoichiometries. All cocrystals were characterized by FT-IR and DSC (SI). A comparison of the simulated XRPD patterns of the single crystals with the XRPD patterns of the milled samples showed a good match in all cases. In all cocrystals, the imidic tautomeric form of ctz (Figure 1) was observed, as found in the X-ray structure of ctz itself.[27] The crystal structures are shown in Figures 3 – 8 and S15 – S18, the hydrogen bond parameters are presented in Table 3.

Crystal Structures

Ctz·dmf. The single crystal structure of the dmf solvate confirmed the previous structure solution from X-ray powder data.[26] Hydrogen bonds between one of the amino protons of the primary amino group and the ring sulfonamide nitrogen ($NH_{sulfonamide}\cdots N(SO_2)=C$) generate a 1D chain of ctz molecules. The chains are connected through $NH_{sulfonamide}\cdots O$ and $NH_{thiadiazine}\cdots O$ hydrogen bonding involving the dmf oxygen. The $NH_{sulfonamide}\cdots N(SO_2)=C$ synthon is also the predominant synthon in the structure of solvent-free ctz.[27] In addition, $NH_{thiadiazine}\cdots O=S$ and $NH_{sulfonamide}\cdots O=S$ interactions are observed in solvent-free ctz which are replaced by the $NH\cdots O_{amide}$ H bonds in ctz·dmf.

Ctz-bipy. The asymmetric unit comprises one ctz molecule and half a bipy molecule. In the crystal packing four ctz molecules and two bipy molecules are linked through $NH_{sulfonamide}\cdots N_{py}$ and $NH_{sulfonamide}\cdots N_{thiadiazine}$ hydrogen bonds into a supramolecular ring structure (graph set notation $R_6^6(38)$). The 3D structure is further stabilized by $NH_{thiadiazine}\cdots O=S$ and $CH_{thiadiazine}\cdots O=S$ interactions.

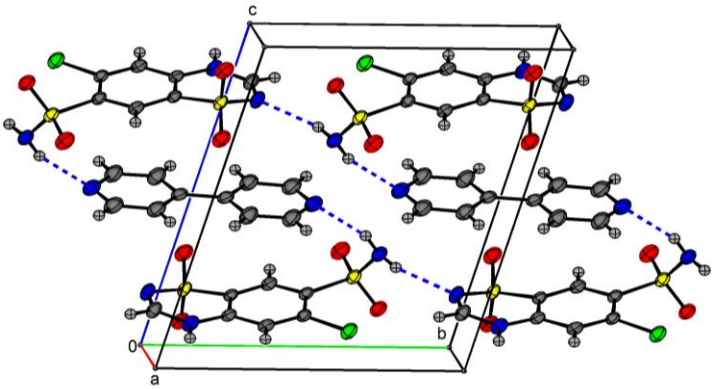

Figure 3. $R_6^6(38)$ motif in ctz-bipy.

Ctz-ebipy. There are one ctz molecule and one ebipy molecule in the asymmetric unit. One pyridine nitrogen of ebipy participates in H bonding with two primary sulfonamide groups ($NH_{sulfonamide}\cdots N_{py}$) while the second one interacts with the thiadiazine NH of ctz. Overall, an interwoven 2D layer structure is formed with $R_4^4(38)$ and $R_4^2(8)$ rings both built up by two ctz and two ebipy molecules. In contrast to ctz-bipy, none of the sulfonyl oxygens acts as a NH hydrogen bond acceptor and the ctz molecules do not hydrogen bond with each other.

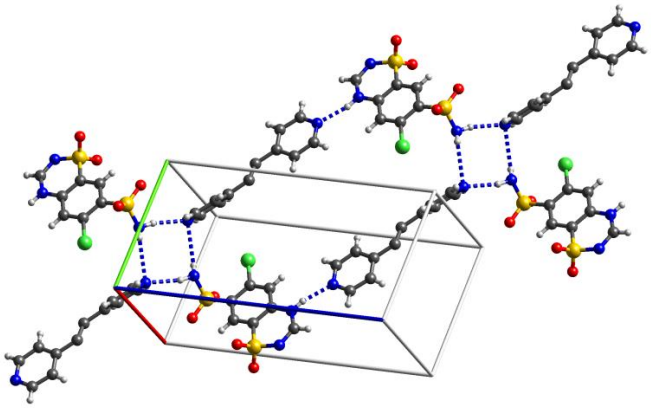

Figure 4. $R_4^2(8)$ and $R_4^4(38)$ motifs in ctz-ebipy.

Ctz-pbipy. The bipyridyl coformer with a propyl linker between the two pyridines gives a cocrystal with 1:2 stoichiometry. One pbipy is involved in $NH_{sulfonamide}\cdots N_{py}$ and $NH_{thiadiazine}\cdots N_{py}$ hydrogen bonding. These H bonds lead to $R_4^4(40)$ rings. Noteworthy, the other pbipy has unused H bond acceptor capacity, as only one of the two pyridine groups interacts with ctz ($NH_{sulfonamide}\cdots N_{py}$). As in the case of ctz-ebipy there are no H bond interactions between ctz molecules.

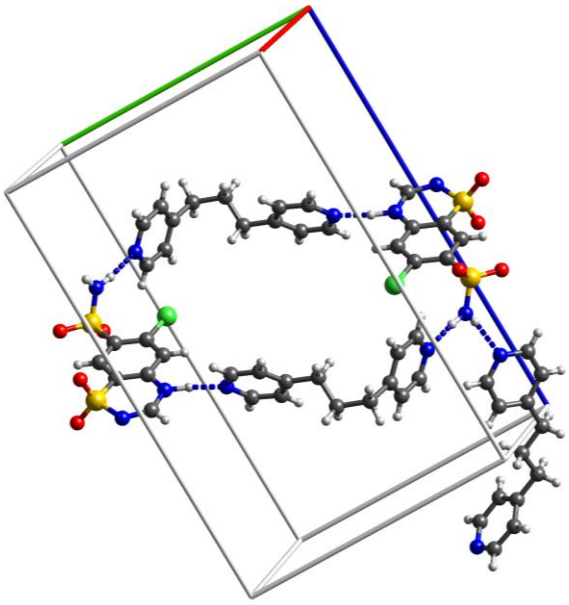

Figure 5. $R_4^4(40)$ motif in ctz-pbipy.

Ctz-hma. The asymmetric unit of ctz-hma contains one molecule of ctz, one molecule of hma and one solvent molecule (CH_3CN). Ctz and hma assemble into a 3D supramolecular structure *via*

$NH_{sulfonamide}\cdots N_{amine}$ and $NH_{thiadiazine}\cdots N_{amine}$ hydrogen bonding. Three of the four amine nitrogens of hma serve as H bond acceptors while the fourth hma nitrogen presents unused H bond acceptor capacity.

Ctz-bza. The ctz molecules are connected into 1D double chains through pairwise $NH_{sulfonamide}\cdots O{=}S$ hydrogen bonds between the primary sulfonamide and the ring sulfonamide groups. The chains are linked into a 3D supramolecular network by bza which forms H bonds with the thiadiazine ring nitrogens ($NH_{thiadiazine}\cdots O_{amide}$, $NH_{amide}\cdots N(SO_2){=}C$). Noteworthy, only one of the bza amide protons participates in hydrogen bonding.

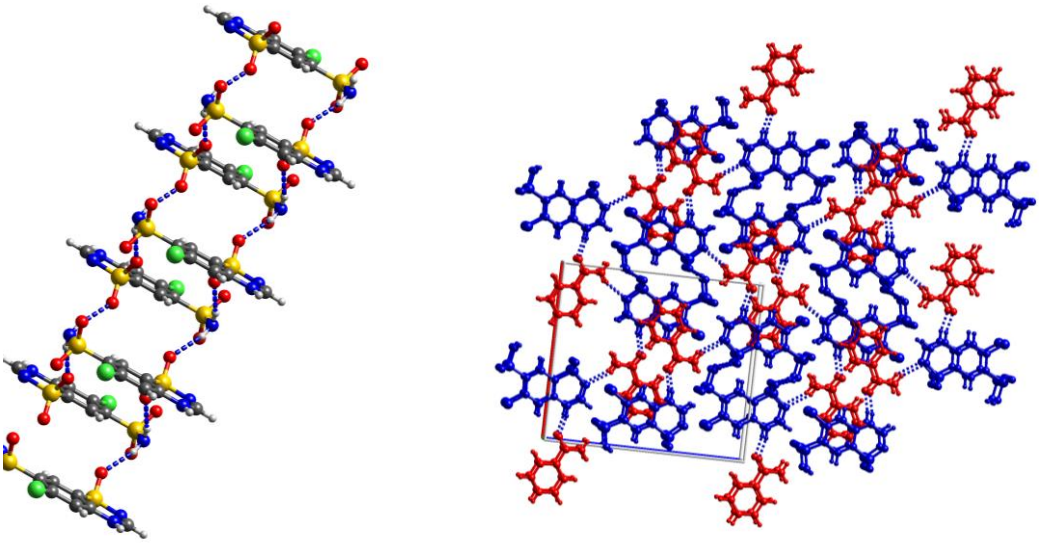

Figure 6. 1D chain of ctz molecules in ctz-bza and extension into a 3D supramolecular structure by bza.

Ctz-cbz. Ctz and cbz cocrystallize in a 1:2 stoichiometry. The asymmetric unit comprises four crystallographically independent cbz molecules, two ctz molecules, one acetone and one water molecule of crystallization. The two crystallographically independent ctz molecules differ in the orientation of their sulfonamide group relative to the sulfur of the thiadiazine ring (see below). The cbz molecules are present as dimers with the typical $R_2^2(8)$ amide homosynthon. The dimers are linked by two ctz molecules *via* $NH_{thiadiazine}\cdots O_{amide}$ and $NH_{amide}\cdots O{=}S$ interactions into an infinite chain. The primary sulfonamide group forms H bonds with sulfonyl oxygen and the oxygen of the acetone of crystallization. The water molecule of crystallization is involved in H bonding with the sulfonyl oxygen and acetone.

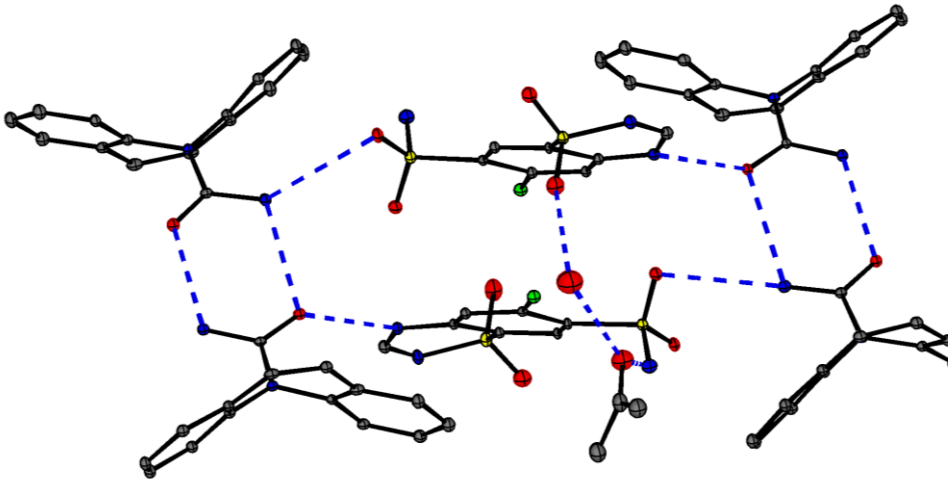

Figure 7. Hydrogen bonding in ctz-cbz.

Ctz-ina. The coformer ina contains two groups with hydrogen bonding capability, the pyridyl nitrogen and the amide group. The cocrystal with ctz has a 1:1 stoichiometry and features the $NH_{sulfonamide}\cdots N_{py}$ heterosynthon already found in ctz-bipy, ctz-ebipy and ctz-pbipy. Furthermore, $NH_{amide}\cdots N(SO_2)=C$ and $NH_{amide}\cdots O=S$ hydrogen bonding is observed. The amide oxygen of ina serves as a bifurcated acceptor by forming hydrogen bonds with the primary sulfonamide group and with $NH_{thiadiazine}$. In contrast to ctz-cbz, the $R_2^2(8)$ amide homosynthon is absent.

Ctz-nia. The asymmetric unit of ctz-nia consists of two ctz molecules (denoted as **A** and **B**), two nia molecules (denoted as **a** and **b**) and two water molecules of crystallization. The ctz-**A** molecules form intermolecular $NH_{sulfonamide}\cdots O=S_{primary}$ H bonds. The sulfonamide protons additionally hydrogen bond to the amide oxygens of two adjacent nia-**a** molecules. The NH···O sulfonamide-amide heterosynthon is also formed by ctz-**B**. Further H bonding occurs between the $NH_{thiadiazine}$ of ctz-**A** and ctz-**B** and water of crystallization. The amide nitrogen of nia-**a**/**b** donates a hydrogen bond to sulfonyl oxygen. $HOH\cdots N_{py}$ interactions are observed for one of the two crystallographically independent nia molecules. The pyridine nitrogen of the second one (nia-**b**) participates in $C\text{-}H\cdots N_{py}$ H bonding. The 3D structure is further stabilized by H bonding between the water of crystallization and sulfonyl oxygen and CH···N and CH···O interactions.

(bzamH$^+$)(ctz$^-$). The X-ray structure shows that proton transfer from the thiadiazine ring of ctz to bzam has taken place. Two ctz anions assemble into dimers with a face-face arrangement through pairwise $NH_{sulfonamide}\cdots O=S_{ring}$ hydrogen bonds ($R_2^2(16)$ motif). There are also short C-Cl···O=S contacts between the ctz anions within the dimers. Adjacent dimers associate through

$NH_{sulfonamide}$···O=S interactions involving the second oxygen of the ring sulfonyl group. The amidinium group of the $bzamH^+$ cation forms charge-assisted H bonds with the deprotonated thiadiazine nitrogen, with the sulfonyl oxygen and $N(SO_2)$=C nitrogen which extends the structure into a 3D network.

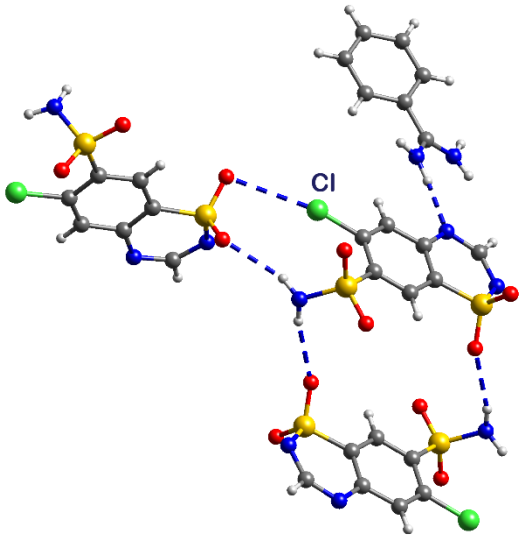

Figure 8. Hydrogen bonding in (bzamH+)(ctz^-).

Hydrogen bonding and conformational analysis. Ctz contains five H bond acceptors, the thiadiazine nitrogen, the two oxygens of the primary sulfonamide group and the two oxygens of the endocyclic sulfur, and two types of H bond donor, the amino protons of the primary sulfonamide group and the proton on the ring nitrogen. Only one polymorph and an isosymmetric high pressure phase are known in which the sulfonamide amino group forms N-H···O and NH···N hydrogen bonds with sulfonamide oxygens and with the thiadiazine nitrogen.[27-29] The $NH_{sulfonamide}$···O=S homosynthon is maintained in ctz-bza, ctz-nia and in the benzamidinium salt. The $NH_{sulfonamide}$···$N_{thiadiazine}$ catemer homosynthon of ctz is retained in ctz-bipy, while in all other cocrystals a pyridyl nitrogen, amine nitrogen or amide oxygen competes for the primary sulfonamide group.

To further analyze and understand the cocrystallization behavior of ctz, a motif search in the CSD was carried out. 3644 structures with motif I (Figure 2) were found out of which 865 belong to the subset Ia. Bifurcated NH_2···$N_{pyridyl}$ H bonding (motif II) is less common with 49 hits. Out of the 865 entries with motif Ia, 501 were single molecule species and 297 were cocrystals, salts or solvates. A specific search for sulfonamides revealed 111 structures with motif I'. Subset Ia' gave 28 hits. In line with

this, four of the five coformers containing pyridine nitrogen – bipy, ebipy, pbipy and ina – gave cocrystals with ctz with heterosynthon Ia'.

Motif III is found in ctz·dmf and ctz-bipy ($NH_{sulfonamide}\cdots N(SO_2)=C$) as well as in ctz-ina and ctz-bza ($NH_{amide}\cdots N(SO_2)=C$). Otherwise, the imidic nitrogen does not participate in H bonding which is in line with the CSD search that gave 82 entries for synthon III only 12 of which are cocrystals.

All amides used in the screening study gave cocrystals with ctz. In three of the five structurally characterized ctz-amide cocrystals/solvate $NH_{sulfonamide}\cdots O_{amide}$ hydrogen bonds are present, while the thiadiazine NH nitrogen acts as H bond donor for the amide oxygen in all cases except for ctz-nia where $NH_{thiadiazine}$ interacts with water of crystallization. For three of the four cocrystals with a primary amide coformer $NH_{amide}\cdots O=S$ interactions are observed. $NH_{thiadiazine}\cdots O=S$ bonds occur only in ctz·dmf. There are 208 entries for bifurcated hydrogen bonding between the amide group and X_2N-H (motif IV) in the CSD. However, this H bonding pattern is observed in none of the ctz-amide cocrystals.

It is surprising that no cocrystals could be obtained with a carboxylic acid coformer. The same observation has been made in cocrystallization experiments of sulfacetamide.[16] The CSD has 297 entries for cocrystals, salts, and solvates that contain motif Ia. In several of these carboxyl groups are present in addition to the pyridine and amine groups of the motif. It seems that in such a case H bonding between the carboxyl group and an amino nitrogen only occurs, when the carboxylic acid has electron-withdrawing substituents or another H bond forming group. REF codes MELYEI, KIXCOK, PICLOE and OFUZUK are examples for this. On this basis, ctz may have been expected to form a cocrystal with nicotinic acid which, however, was not the case.

For X_2N-H/COOH interactions, four different motifs are found (motifs V – VIII) with motifs VI (1 hit), VII (19 hits) and VIII (124 hits) applying to the specific case where X_2N-H is a sulfonamide. Out of the 124 structures with motif VIII only 18 are cocrystals. In all 18 examples the carboxylic acid has an electron-withdrawing substituent or another group with H bonding potential. Furthermore, cocrystal formation of hydrochlorothiazide (HCTZ) with nicotinic acid and with *p*-aminobenzoic acid has recently been reported.[17] Nicotinic acid adopts its zwitterionic form and the hydrochlorothiazide-nicotinic acid cocrystal is sustained by charge-assisted $COO^-\cdots HN_{sulfonamide}$ interactions. However, no cocrystals could be obtained with isonicotinic and salicylic acids, similar to our observations with ctz.

The conformational variability of ctz has been discussed in the literature. Florence and coworkers identified five conformational minima (termed minpa, minsa, minst, minoa and minot, where o, p, and s stand for opposite, parallel and same side to the ring sulfur and a and t stand for the NH_2 protons pointing away from or towards the molecule) by *ab initio* optimization of the isolated molecule structure and found a good agreement with the experimentally observed conformations of the

sulfonamide side chain in the crystal structures of ctz solvates.[29] All five conformers are represented in the cocrystal structures (Table S2, SI). The crystallographically imposed parallel orientation of the sulfonamide side chain relative to the ring sulfur in ctz-bza results in a staircase-like arrangement of the chain of ctz molecules in this cocrystal.

It is interesting to consider why CTZ appears to have a lower co-crystal forming ability than its hydrogenated derivative HCTZ in which the C=N ring double bond is hydrogenated. In particular CTZ failed to form co-crystals with any of the carboxylic acids examined here some of which have been reported to form co-crystals with HCTZ.[17] The possibility that the HCTZ co-crystal forming ability might be due to a more flexible heterocyclic ring was examined. The structures of the thirteen co-crystals reported for HCTZ[17] were fitted using the aromatic ring carbons and compared to fitting of the nine CTZ structures reported here (Figure 9). The range of heterocyclic ring conformations displayed in both series are similar which suggests similar heterocyclic ring rigidities. The frequencies of the heterocyclic ring deformation modes have also been calculated for CTZ and HCTZ and the values 316 cm^{-1} and 262 cm^{-1} are also quite close. However, the presence of an axial N-H hydrogen bond donor in the HCTZ heterocyclic ring has been noted. [29] It is the presence of this hydrogen bond donor that provides an important interaction normal to the molecular plane in the HCTZ co-crystals with both nicotinic acid and *p*-aminobenzoic acid neither of which form co-crystals with CTZ.

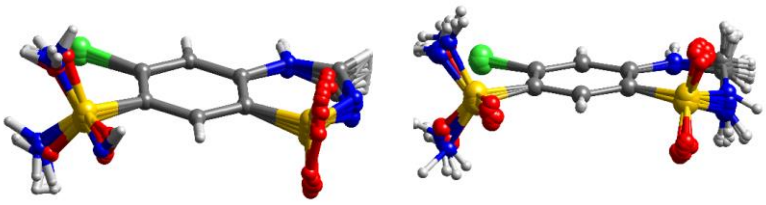

Figure 9. Fitting of the CTZ molecules from the structures in Table 1 using the six aromatic carbons and fitting of the HCTZ molecules from the thirteen reported co-crystal structures using their six aromatic carbons.

Thermal behavior

The thermal behavior of the cocrystals was studied by DSC and the thermograms are displayed in Figures S19 – S27 (SI). In the case of ctz-bza and ctz-ina the melting endotherm of the coformer is observed as the first thermal event at 125.8 and 157.3 °C, respectively. The DSC plot of ctz-nia shows an endothermic event at 118.1 °C which is followed by melting of ina at 129.6 °C. Ctz-hma, ctz-cbz, ctz-pbipy and ctz-bipy give endotherms at 192.5, 155.8, 130.1 and 228.2 °C, respectively, distinct

from the melting temperature of either ctz (350 °C) or hma (280 °C), cbz (190 °C), pbipy (57-60 °C) or bipy (114 °C) confirming the thermal stability of the new phases. Generally, for a cocrystal a melting point in between the melting points of the two components is expected. In our series of cocrystals this is only the case for ctz-bipy and ctz-pbipy. The DSC plot of ctz-ebipy features a peak at 104.4 °C followed by a peak at 151.5 °C corresponding to the melting point of ebipy. The benzamidinium salt melts at 221.4 °C.

Dissolution studies

The dissolution behavior is an important physicochemical property that has a direct impact on the bioavailability of a drug. The dissolution behavior can be modulated by cocrystal formation and both an increase and a decrease in the dissolution properties has been reported for cocrystals compared to the pure API.[16,30-35] The dissolution profiles of the cocrystals and the benzamidinium salt were measured and are shown in Figures 10 and S28.

Enhanced dissolution properties were observed for ctz-cbz, ctz-ebipy and ctz-pbipy. Ctz-hma, ctz-bipy, ctz-nia, ctz-bza and ctz-ina have similar or lower dissolution properties than ctz. The stability of the cocrystals in the dissolution medium was checked by XRPD after recovering the undissolved residue by filtration at the end of the dissolution measurement. Ctz-bipy and ctz-ebipy were found to be stable in the dissolution medium, while ctz-pbipy, ctz-hma, ctz-cbz, ctz-ina, ctz-nia and ctz-bza dissociate into the separate components, as evident from the XRPD patterns. Cbz is polymorphic and the cocrystal converts to the channel solvate form II. Somewhat unexpectedly, the benzamidinium salt gave the same dissolution profile as ctz. The XRPD pattern showed the Bragg peaks of ctz indicating that the ctz salt converts back to neutral ctz on contact with buffer.

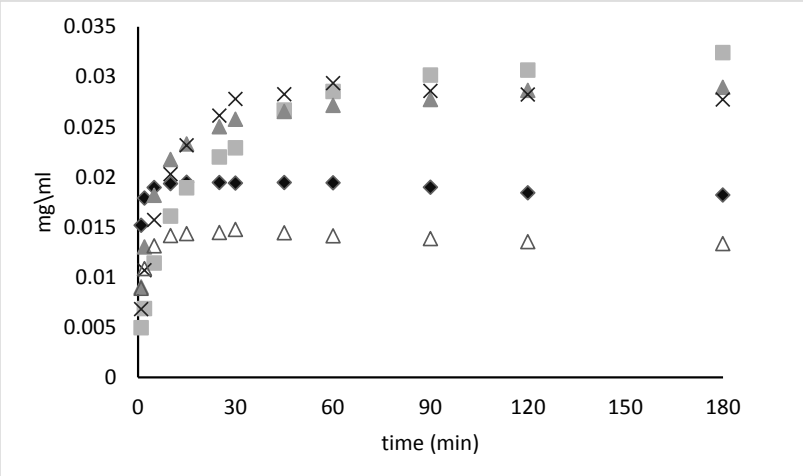

Figure 10. Powder dissolution profiles of ctz (♦), ctz-cbz (■), ctz-ebipy (▲), ctz-pbipy (×) and ctz-ina (Δ). Phosphate buffer (pH 6.8), 37 °C.

Cocrystal formation is associated with shifts of characteristic IR bands and the change in wavenumber $\Delta\nu$ is an indicator for the relative strength of the H bonding interaction between the functional groups of the two components. The symmetric and asymmetric stretching vibrations of the exocyclic and endocyclic SO_2 groups in ctz give broad bands at 1161 cm^{-1} and 1303/1345 cm^{-1}, respectively. The ν(N-H) vibrations of the sulfonamide group appear a 3325 and 3238 cm^{-1}. In ctz-pbipy, ctz-ebipy, ctz-hma, ctz-nia and ctz-bipy the broad band at 1161 cm^{-1} splits into two sharp bands at 1142-1155 and 1165-1172 cm^{-1} (SI), while the $\nu_{as}(SO_2)$ bands are shifted by -15 to +6 cm^{-1}. However, no correlation between $\Delta\nu$ and the stability in the dissolution medium or the dissolution rate was apparent.

In an effort to correlate the observed dissolution rates with crystal lattice stability the lattice energy has been estimated using the PIXEL program[36] and the crystal packing index has also been calculated. The results obtained and the dissolution at 60 min. are listed in Table 4. The pixelc program can only be applied to structures with two or less molecules in the asymmetric unit and the more approximate clpcry program could not be applied to some of the more complex asymmetric units. One of the highest dissolution rates was shown by the pbipy cocrystal which has the lowest packing index and the lowest clpcry lattice energy. In contrast, the poorly dissolving ina cocrystal has a relatively high clpcry lattice energy and the highest packing index. The high dissolution rate of ctz-ebipy is more difficult to rationalize, as this cocrystal has a relatively high packing index and clpcry lattice energy. Noteworthy, ctz-ebipy is one of the two cocrystals that are stable in the dissolution medium and do not convert to ctz. Ctz-bza has a low packing index and lower lattice energy, but gives no dissolution advantage over ctz. Ctz-bza is the only cocrystal in which pairwise $NH_{sulfonamide}\cdots O{=}S$ hydrogen bonds link the ctz molecules into a double chain. The bipy cocrystal maintains the $NH_{sulfonamide}\cdots N(SO_2){=}C$ homosynthon of ctz and also shows a low dissolution rate.

Conclusions

The first cocrystals and a salt of chlorothiazide have been obtained by ball milling and crystallization from solution. XRPD patterns indicate that thirteen coformers gave cocrystals on milling and it was possible to crystallize eight cocrystals and a salt from solution. A motif search of the CSD using ctz complementary synthons suggested that N based H-bond acceptors and carboxylic acids rarely form ctz cocrystals and in agreement with predictions carboxylic acid coformers gave no indication of cocrystal formation.

One of the cocrystals maintains the 1D motif observed in the ctz form I structure ($NH_{sulfonamide}\cdots N(SO_2){=}C$), while the $NH_{sulfonamide}\cdots O{=}S$ synthon is preserved in three of the cocrystals and the salt.

The dissolution behavior of the ctz cocrystals appears to be mainly determined by the cocrystal lattice energy as there is a correlation between the crystal packing index, lattice energy and dissolution rate, but the presence or absence of ctz homosynthons also plays a role.

Acknowledgement

This work was supported by Science Foundation Ireland under Grant No. [12/RC/2275] as part of the Synthesis and Solid State Pharmaceutical Centre (SSPC). M.A. acknowledges the Royal Embassy of Saudi Arabia for a Saudi Arabia Government Scholarship.

Supporting Information Available

Figures of the X-ray structures of ctz·dmf, ctz-hma and ctz-ina; measured and calculated XRPD patterns, IR data of the cocrystals, DSC plots.

Accession Codes

CCDC 1551836 (ctz-bipy), 1551880 (ctz·dmf), 1551879 (ctz-bza), 1551881 (ctz-pbipy), 1551885 (ctz-ebipy), 1551886 (ctz-cbz), 1551887 (ctz-hma), 1551888 (ctz-ina), 1551889 (ctz-nia), 1551899 ((bzamH$^+$)(ctz$^-$)) contain the supplementary crystallographic data for this paper. These data can be obtained free of charge via www.ccdc.cam.ac.uk/data_request/cif, or by emailing data_request@ccdc.cam.ac.uk, or by contacting The Cambridge Crystallographic Data Centre, 12 Union Road, Cambridge CB2 1EZ, UK; fax: +44 1223 336033.

References

(1) Kale, D. P.; Zode, S. S.; Bansal, A. K. *J. Pharm. Sci*. **2017**, *106*, 457–470.

(2) Bolla, G.; Nangia, A. *Chem. Commun*. **2016**, *52*, 8342–8360.

(3) Blagden, N.; Coles, S. J.; Berry, D. J. *CrystEngComm* **2014**, *16*, 5753–5761.

(4) Schultheiss, N.; Newman, A. Cryst. *Growth Des*. **2009**, *9*, 2950–2967.

(5) Trask, A. V. *Mol. Pharmaceutics* **2007**, *4*, 301–309.

(6) Thakuria, R.; Delori, A.; Jones, W.; Lipert, M. P.; Roy, L.; Rodriguez-Hornedo, N. *Int. J. Pharm*. **2013**, *453*, 101–125.

(7) Qiao, N.; Li, M.; Schlindwein, W.; Malek, N.; Davies, A.; Trappitt, G. *Int. J. Pharm*. **2011**, *419*, 1–11.

(8) Adsmond, D. A.; Grant, D. J. W. *J. Pharm. Sci*. **2001**, *90*, 2058–2077.

(9) Hu, Y.; Gniado, K.; Erxleben, A.; McArdle, P. *Cryst. Growth Des*. **2014**, *14*, 803–813.

(10) Ghosh, S.; Bag, P. P.; Reddy, C. M. *Cryst. Growth Des*. **2011**, *11*, 3489–3503.

(11) Goud, N. R.; Babu, N. J.; Nangia, A. *Cryst. Growth Des*. **2011**, *11*, 1930–1939.

(12) Suresh, K.; Minkov, V. S.; Namila, K. K.; Derevyannikova, E.; Losev, E.; Nangia, A.; Boldyreva, E. V. *Cryst. Growth Des*. **2015**, *15*, 3498–3510.

(13) Bolla, G.; Mittapalli, S.; Nangia, A. *CrystEngComm* **2014**, *1*6, 24–27.

(14) Gopi, S. P.; Banik, M.; Desiraju, G. R. *Cryst. Growth Des*. **2017**, *17*, 308–316.

(15) Banik, M.; Gopi, S. P.; Ganguly, S.; Desiraju, G. R.; *Cryst. Growth Des*. **2016**, *1*6, 5418–5428.

(16) Goud, N. R.; Khan, R. A.; Nangia, A. C*rystEngComm* **2014**, *16*, 5859–5869.

(17) Sanphui, P.; Rajput, L. *Acta Cryst*. **2014**, *B70*, 81–90.

(18) MacFhionnghaile, P.; Hu, Y.; Gniado, K.; Curran, S.; McArdle, P.; Erxleben, A. *J. Pharm. Sci*. **2014**, *103*, 1766–1778.

(19) Ernst, M. E.; Grimm, R. H., Jr. *Curr. Hypertens. Rev*. **2008**, *4*, 256–265.

(20) Lu, T.; Chen, C. Measurement, **2007**, *40*, 591–599.

(21) McArdle, P.; Gilligan, K.; Cunningham, D.; Dark, R.; Mahon, M. *CrystEngComm* **2004**, *6*, 303–309.

(22) (a) SHELXT - Sheldrick, G. M. *Acta Crystallogr*. 2015, *A71*, 3-8. (b) SHELXL - Sheldrick, G. M. *Acta Crystallogr*. **2015**, *C71*, 3–8.

(23) Bruno, I. J.; Cole, J. C.; Edgington, P. R.; Kessler, M.; Macrae, C. F.; McCabe, P.; Pearson, J.; Taylor, R. *Acta Cryst*. **2002**, *B58*, 389–397.

(24) Pallipurath, A. R.; Civati, F.; Eziashi, M.; Omar, E.; McArdle, P.; Erxleben, A. *Cryst. Growth Des*. **2016**, *16*, 6468–6478.

(25) Granovsky, A. A. Firefly (previously PC GAMESS) 2017. http://classic.chem.msu.su/gran/firefly/index.html

(26) Fernandes, P.; Florence, A. J.; Shankland, K.; Shankland, N.; Johnston, A. *Acta Cryst., Section E: Structure Reports Online* **2006**, *62*, o2216–o2218.

(27) Shankland, K.; David, W. I. F.; Silva, D. S. *J. Mater. Chem*. **1997**, *7*, 569–572.

(28) Oswald, I. D. H.; Lennie, A. R.; Pulham, C. R.; Shankland, K. *CrystEngComm* **2010**, *12*, 2533–2540.

(29) Johnston, A.; Bardin, J.; Johnston, B. F.; Fernandes, P.; Kennedy, A. R.; Price, S. L.; Florence, A. J. *Cryst. Growth Des*. **2011**, *11*, 405–413.

(30) Jung, M. S.; Kim, J. S.; Kim, M. S.; Alhalaweh, A.; Cho, W.; Hwang, S. J.; Velaga, S. P. *J. Pharm. Pharmacol.* **2010**, *62*, 1560−1568.

(31) McNamara, D. P.; Childs, S. L.; Giordano, J.; Iarriccio, A.; Cassidy, J.; Shet, M. S.; Mannion, R.; O'Donnell, E.; Park, A. *Pharm. Res*. **2006**, *23*, 1888−1897.

(32) Smith, A. J.; Kavuru, P.; Wojtas, L.; Zaworotko, M. J.; Shytle, R. D. *Mol. Pharmaceutics* **2011**, *8*, 1867−1876.

(33) Hickey, M. B.; Peterson, M. L.; Scoppettuolo, L. A.; Morrisette, S. L.; Vetter, A.; Guzman, H.; Remenar, J. F.; Zhang, Z.; Tawa, M. D.; Haley, S.; Zaworotko, M. J.; Almarsson, O. *Eur. J. Pharm. Biopharm*. **2007**, *67*, 112−119.

(34) Cheney, M. L.; Weyna, D. R.; Shan, N.; Hanna, M.; Wojtas, L.; Zaworotko, M. J. *J. Pharm. Sci*. **2011**, *100*, 2172−2181.

(35) Smith, A. J.; Kavuru, P.; Arora, K. K.; Kesani, S.; Tan, J.; Zaworotko, M. J.; Shytle, R. D. *Mol. Pharmaceutics* **2013**, *10*, 2948–2961.

(36) Gavezzotti, A. *Z. Kristallogr.* **2005**, *220*, 499–510.

Table 1. Crystallographic data of ctz·dmf, ctz-bipy, ctz-ebipy, ctz-pbipy and ctz-hma

	ctz·dmf	**ctz-bipy**	**ctz-ebipy**	**ctz-pbipy**	**ctz-hma**
Formula	$C_{10}H_{13}ClN_4O_5S_2$	$C_{12}H_{10}ClN_4O_4S_2$	$C_{19}H_{16}ClN_5O_4S_2$	$C_{33}H_{34}ClN_7O_4S_2$	$C_{15}H_{21}ClN_8O_4S_2$
M_r	368.81	373.81	477.94	692.24	476.97
Crystal colour and habit	colorless block	colorless block	colorless block	colorless block	colorless block
Crystal size (mm)	0.5 × 0.4 × 0.2	0.5 × 0.4 × 0.2	0.5 × 0.2 × 0.15	0.5 × 0.2 × 0.2	0.5 × 0.4 × 0.2
Crystal system	triclinic	triclinic	triclinic	monoclinic	monoclinic
Space group	P-1	P-1	P-1	$P2_1/c$	$P2_1/c$
Unit cell dimensions					
a [Å]	8.0926(9)	6.3561(5)	6.8063(4)	13.1953(7)	7.3113(6)
b [Å]	8.9880(9)	9.9537(8)	9.0058(6)	12.6162(8)	20.6107(15)
c [Å]	11.2828(10)	12.4037(9)	16.6206(12)	20.5137(10)	13.4601(11)
α [°]	85.873(7)	71.806(7)	87.555(6)		
β [°]	74.301(9)	79.256(6)	81.389(6)	96.473(5)	91.624(8)
γ [°]	72.514(9)	76.929(7)	83.085(5)		
V [Å^3]	753.51(14)	720.48(10)	999.65(12)	3393.2(3)	2027.5(3)
Z	2	2	2	4	4
D_{calc} (g cm^{-3})	1.626	1.723	1.588	1.355	1.563
No. measd. reflections	5512	5330	6061	16530	9285
no. unique reflections (R_{int})	3396	3264	3618	7849	4706
No. obs. reflections	2701	2723	2214	3512	3451
Final R_1, wR_2 (obs. refl.)	3.8 %, 9.9 %	4.6 %, 8.9 %	4.7 %, 10.6 %	7.0 %, 10.9 %	5.1 %, 11/3 %
Goodness-of-fit (obs. refl.)	1.058	1.050	0.923	0.966	1.060

Table 2. Crystallographic data of ctz-bza, ctz-cbz, ctz-nia, ctz-ina and ($bzamH^+$)(ctz^-)

	ctz-bza	**ctz-cbz**	**ctz-nia**	**ctz-ina**	**($bzamH^+$)(ctz^-)**
Formula	$C_7H_{6.5}Cl_{0.5}N_2O_{2.5}S$	$C_{77}H_{68}Cl_2N_{14}O_{14}S_4$	$C_{13}H_{14}ClN_5O_6S_2$	$C_{13}H_{12}ClN_5O_5S_2$	$C_{14}H_{14}ClN_5O_4S_2$
M_r	416.85	1612.59	435.82	417.85	415.87
Crystal colour and habit	colorless block	colorless block	colorless block	colorless block	colorless block
Crystal size (mm)	0.5 × 0.4 × 0.2	0.5 × 0.4 × 0.2	0.5 × 0.4 × 0.2	0.5 × 0.4 × 0.2	0.5 × 0.4 × 0.2
Crystal system	orthorhombic	orthorhombic	monoclinic	monoclinic	monoclinic
Space group	Pnma	$Pca2_1$	$P2_1/c$	$P2_1/n$	$P2_1/n$
Unit cell dimensions					
a [Å]	15.0955(7)	10.3190(6)	17.1278(10)	8.9743(5)	9.7594(4)
b [Å]	6.7476(4)	27.1654(16)	8.1039(3)	17.4518(7)	10.8648(4)
c [Å]	16.9811(8)	26.906(2)	25.1983(12)	10.2741(5)	16.2997(5)
β [°]			95.546(5)	94.734(5)	91.397(3)
V [$Å^3$]	1729.67(15)	7542.3(8)	3481.2(3)	1603.62(14)	1727.81(11)
Z	4	4	8	4	4
D_{calc} (g cm^{-3})	1.601	1.420	1.663	1.731	1.599
No. measd. reflections	13294	21741	16515	6768	7706
no. unique reflections (R_{int})	2320	10692	8179	3685	3993
No. obs. reflections	1905	6833	4247	2801	3177
Final R_1, wR_2 (obs. reflections)	4.4 %, 10.6 %	9.4 %, 23.3 %	6.9 %, 15.0 %	4.4 %, 11.0 %	3.9 %, 9.5 %
Goodness-of-fit (obs. reflections)	1.079	1.051	1.012	1.002	1.070

Table 3. Hydrogen bonding distances and angles

D-H···A	d(D···A) (Å)	∠(DHA) (°)	symmetry code
ctz.dmf			
N2-H...O5	2.734(3)	171(3)	x,y,z
N3-H...N1	3.130(3)	162(3)	-1+x,1+y,z
N3-H...O5	2.882(3)	158(3)	-1+x,y,1+z
C1-H...O4	3.242(3)	136.00	1-x,1-y,1-z
ctz-bipy			
N3-H...N1	3.098(3)	160(3)	x,1+y,z
N2-H2...O1	2.841(2)	149.00	1+x,y,z
N3-H...N4	2.874(3)	155(3)	x,y,z
C1-H...O4	3.371	163.00	1+x,-1+y,z
ctz-ebipy			
N2-H...N4	2.843(4)	168.00	1-x,1-y,1-z
N3-H...N5	2.937(4)	165(4)	1-x,-y,-z
N3-H...N5	3.237(4)	134(3)	x,1+y,z
C17-H...O2	3.466(4)	160.00	-x+2,-y+2,-z+1
C19-H...O1	3.492(4)	170.00	-x+1,-y+1,-z+1
ctz-pbipy			
N3-H...N6	2.918(4)	163(3)	x,y,z
N3-H...N5	2.871(5)	172(3)	1-x,1-y,1-z
N2-H...N4	2.779(4)	154(3)	x,y,z
C17-H...O1	3.318(5)	152.00	x,1/2-y,-1/2+z
C18-H...O3	3.414(5)	147.00	x,1/2-y,-1/2+z
C21-H...O3	3.332(5)	150.00	1-x,1/2+y,3/2-z
C24-H...O2	3.440(5)	152.00	x,-1/2-y,1/2+z
ctz-hma			
N3-H...N6	3.055(3)	146(3)	-x,-1/2+y,1/2-z
N3-H...N4	3.103(3)	166(3)	-x,1-y,1-z
N2-H...N5	2.845(3)	167(3)	x,y,z
C9-H...O2	3.500(3)	156.00	1-x,1/2+y,1/2-z
C11-H...O3	3.416(3)	149.00	-1+x,y,z
ctz-bza			
N3-H...O1	2.873(3)	167(2)	-x,1/2+y,1-z
N2-H...O3	2.708(3)	167.00	x,y,z
N4-H...N1	3.184(4)	156	1/2+x,3/2-y, 3/2-z
C1-H...O2	3.121(3)	120	1/2-x,1-y,1/2+z
C1-H...O2	3.121(3)	120	1/2-x,1/2+y,1/2+z
ctz-cbz			
N2-H...O11	2.803(10)	163.00	x,y,z
N5-H...O10	2.850(10)	167.00	x,y,z
N8-H...O10	3.165(10)	162.00	x,y,z
N10-H...O9	2.909(10)	161.00	x,y,z
N10-H...O2	3.152(11)	144.00	1/2+x,1-y,z
N12-H...O12	2.940(10)	162.00	x,y,z
N12-H...O6	3.213(10)	146.00	-1/2+x,-y,z
N14-H...O11	3.223(10)	159.00	

C7-H7...O12	3.150(12)	166.00	-1/2+x,-y,z
C14-H...O9	3.184(14)	161.00	1/2+x,1-y,z
O14...O1	2.70(3)		x,y,z
O14...O13	2.97(3)		x,y,z
ctz-ina			
N3-H...O5	2.985(3)	159(3)	3/2-x,1/2+y,3/2-z
N3-H...N4	2.897(3)	175(3)	x,y,z
N2-H...O5	3.324(3)	158(3)	-1/2+x,1/2-y,-1/2+z
N5-H...O1	3.009(3)	167(3)	-1/2+x,1/2-y,-1/2+z
N5-H...N1	3.078(3)	176(3)	x,-1+x,z
C9-H...O1	3.323(30	161.00	-1/2+x,1/2-y,-1/2+z
ctz-nia			
N1-H...O9	2.884	107.00	x,y,z
N1-H...O1	2.984(5)	111.00	1-x,1/2+y,3/2-z
N1-H...O9	3.036(5)	142.00	1-x,1/2+y,3/2-z
N2-H...O11	2.816(5)	178.00	x,y,z
N4-H...O10	2.889(5)	110.00	x,y,z
N4-H...O10	3.011(5)	146.00	2-x, 1/2+y, 1/2-z
N5-H...O12	2.685(8)	164.00	x,y,z
N5-H...O12B	2.687(8)	174.00	x,y,z
N8-H...O5	3.071(5)	161.00	2-x,-y,1-z
N10-H...O2	3.012(5)	155.00	1-x,1-y,1-z
N7...O12	2.761(8)		x,y,z
N7...O12B	2.704(9)		x,y,z
O12...O7	3.044(8)		x,-1+y,z
O12B...O7	2.938(9)		x,-1+y,z
C1-H...N9	3.228(7)	162.00	x,y,z
C7-H...O3	3.309(6)	161.00	x,1+y,z
C10-H...O7	3.482(6)	167.00	x,1+y,z
C16-H...O1	3.324(6)	165.00	1-x,1/2+y,3/2-z
C25-H...O6	3.329(6)	160.00	2-x, 1/2+y, 1/2-z
$(bzamH^+)(ctz^-)$			
N3-H...O2	3.137(3)	160(3)	-1/2+x,3/2-y,-1/2+z
N3-H...O1	3.048(3)	163(3)	1-x,2-y,1-z
N4-H...N1	3.023(3)	157(3)	1/2-x,-1/2+y,3/2-z
N5-H...N2	2.830(3)	169(2)	x,y,z
N5-H...O2	3.006(3)	158(3)	1-x,1-y,1-z

Table 4. Dissolution rates and crystal packing

	dissolved ctz after 60 min. (mg mL^{-1})	Clpcr (kJmol^{-1})	Pixelc (kJmol^{-1})	packing index
ctz	0.018	-190.1		72.5
ctz-cbz	0.032			67.3
ctz-ebipy	0.028	-162.4	-189.6	71.1
ctz-pbipy	0.027	-137.7		65.8
ctz-bza	0.013	-142.5	-177.5	68.2
ctz-ina	0.013	-155.1	-183.4	73.1
ctz-bipy	0.017			71.9
ctz-nia	0.013			70.7

For Table of Content

A Comprehensive Cocrystal Screening Study of Chlorothiazide

Marwah Aljohani, Anuradha R. Pallipurath, Patrick McArdle,* and Andrea Erxleben*

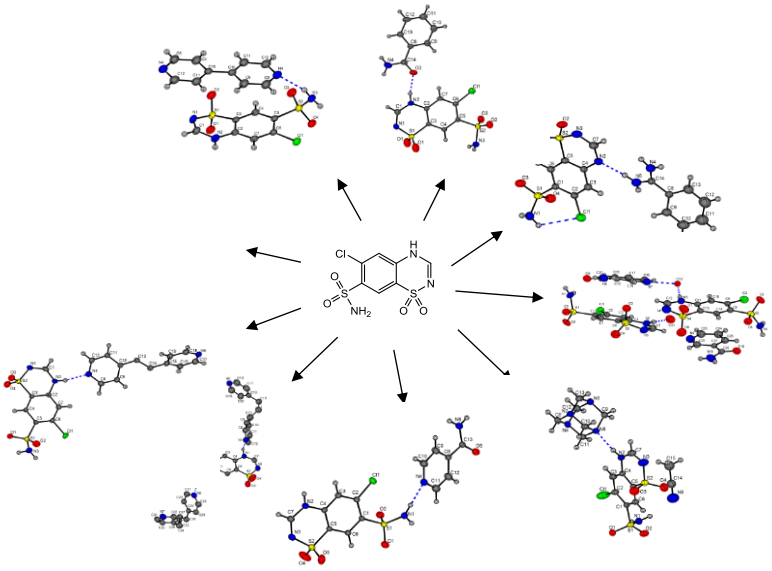

A comprehensive cocrystal screen of the thiadiazine diuretic drug chlorothiazide yielded crystal structures of eight new cocrystals and a salt.